Supporting Information

Reiner et al. 10.1073/pnas.0910001107

SI Text

Kinetic Model. TTET coupled to a local or global conformational transition allows the determination of the equilibrium constant (K_{op}) and of the microscopic rate constants (k_{op} and k_{cl}) for the transition under equilibrium conditions, i.e. without perturbing the system. In addition, the rate constant for loop formation in the unfolded state, k_c, can be obtained (1). Prerequisite for the application of this method is that TTET through loop formation can occur in an unfolded or partially unfolded state (I) but not in the native state (N; see Scheme S1).

This mechanism is essentially identical to hydrogen-deuterium exchange kinetics that allow the determination of stability and dynamics of individual hydrogen bonds in proteins (2, 3).

Different kinetic regimes can be discriminated for TTET coupled to a conformational transition, depending on the relative values of k_{op}, k_{cl}, and k_c. If the equilibrium strongly favors the native state, a single rate constant (λ) for TTET will be observed with

$$\lambda = \frac{k_{op} \cdot k_c}{k_{cl} + k_c}. \qquad [S1]$$

If the conformational transition is much faster than loop formation (k_{cl}, $k_{op} \gg k_c$), Eq. **S1** simplifies to

$$\lambda = \frac{k_{op}}{k_{cl}} \cdot k_c = K_{op} \cdot k_c, \qquad [S2]$$

which corresponds to the EX2-limit in hydrogen exchange. If unfolding is much slower than loop formation, Eq. **S1** becomes

$$\lambda = k_{op}, \qquad [S3]$$

which is the EX1-limit in hydrogen exchange. A shift between the EX1 and the EX2 exchange can occur if a change in experimental conditions has different effects on the different microscopic rate constants. In this case all three microscopic rate constants can be determined.

If both N and I are significantly populated, two apparent rate constants (λ_1 and λ_2) are observed, which are described by the general solution of the three-state model shown in Scheme 1

$$\lambda_{1,2} = \frac{1}{2}(k_{op} + k_{cl} + k_c \pm \sqrt{(k_{op} + k_{cl} + k_c)^2 - 4k_{op} \cdot k_c}) \qquad [S4]$$

with the respective amplitudes

$$A_1 = \frac{1}{\lambda_1(\lambda_1 - \lambda_2)} \cdot ([I]_0 \cdot k_c \cdot (k_{op} - \lambda_1) + [N]_0 \cdot k_{op} \cdot k_c),$$
$$A_2 = \frac{1}{\lambda_2(\lambda_1 - \lambda_2)} \cdot ([I]_0 \cdot k_c \cdot (\lambda_2 - k_{op}) - [N]_0 \cdot k_{op} \cdot k_c). \qquad [S5]$$

If the interconversion between the native and unfolded state is much slower than loop formation (k_{cl}, $k_{op} \ll k_c$), Eq. **S4** simplifies to

$$\lambda_1 = k_c, \qquad \lambda_2 = k_{op}. \qquad [S6]$$

These considerations show that analysis of the observed rate constants and amplitudes of TTET kinetics allows the determination of all microscopic rate constants for a conformational equilibrium with dynamics on a similar timescale or slower than TTET. Because TTET through loop formation occurs on the 10 to 100s of ns timescale, this method allows the probe of transitions that are 10^8 to 10^6 times faster than those accessible to hydrogen exchange. Even in cases when the conformational transition is much slower than the triplet lifetime of the donor, this method allows the determination of rate constant for loop formation in the unfolded state (k_c) when U is populated to as little as 5%, i.e. under native solvent conditions (Eq. **S6**).

Materials & Methods. ***Synthesis, labelling and purification of the HP35 variants.*** The HP35 variants with canonical sequence

H-^{1}LSDEDFKAVF^{11}G**Nle**TRSAFANL
^{21}PL**F**KQQNLKK^{31}EKGLF-OH

were labeled with Xan and Nal at the position indicated in the text. Xan was attached either to the N-terminal amino group of Leu1 (Xan0), to the ϵ-amino group of Lys7, or to the β-amino group of the nonnatural amino acid α,β-diaminopropionic acid replacing Phe35. Nal was introduced either at position 23 or at 35.

All HP35 variants were synthesized using standard 9-fluorenylmethyloxycarbonyl (Fmoc) chemistry on an Applied Biosystems 433A synthesizer. Couplings were performed with HBTU/HOBt or HATU on preloaded Tentagel S PHB-resin (Rapp Polymere). The xanthone derivative 9-oxoxanthene-2carboxylic acid was synthesized according to Graham and Lewis (4), activated with PyBOP and coupled to a selectively deprotected amino functionality. This was either the N-terminal amino group, the ϵ-amino group of Lys7, or the β-amino group of an α,β-diaminopropionic acid incorporated at position 35. In the latter cases, methyltrityl was used as the orthogonal side-chain protection group, which was selectively removed with 3% (v/v) TFA in dichloromethane. Nal was incorporated via Fmoc-protected 1-naphthylalanine (Bachem). Final cleavage from the resin and deprotection of all other side chains was achieved with 94/2/2/2 TFA/TIPS/phenole/H_2O (v/v/v/v). All peptides were purified to >95% purity by preparative HPLC on a RP-8 column. Purity was checked by analytical HPLC and the identity verified by MALDI or electrospray ionization mass spectrometry.

Sample preparation. For all measurements 10 mM potassium phosphate buffer pH 7.0 was used. The concentration of the HP35 variants was determined by the Xan absorption band at 343 nm ($\varepsilon_{343} = 3900\ M^{-1}\ cm^{-1}$). GdmCl and urea concentrations were calculated from the refractive index (5).

TTET experiments. TTET measurements were performed on a laser flash photolysis reaction analyzer (LKS.60) from Applied Photophysics with a Quantel Nd:YAG Brilliant laser. Xanthone triplet states were produced by a 4 ns laserflash at 354.6 nm (~50 mJ). Transient absorption traces were recorded at 590 nm (specific triplet absorbance band of xanthone) to monitor decay of the xanthone triplet state and at 420 nm (specific triplet absorbance band of naphthyl) to monitor formation of the naphthyl triplet state. Peptide concentrations were 50 μM. Absence of

intermolecular TTETwas confirmed by measuring Xan triplet decay of 50 μM donor-only HP35 in the presence of 50 μM acceptor-only HP35. All fitting procedures were performed with ProFit (QuantumSoft).

Temperature dependence of TTET. The temperature dependencies of the rate constants for TTET were measured between 5 and 30 °C and analyzed using the Arrhenius equation

$$k = A \cdot e^{-E_a/RT}, \qquad \text{[S7]}$$

where A represents the preexponential factor and E_A is the activation energy.

The temperature dependence of the equilibrium between N and N′ (Fig. 3) was fitted using the van't Hoff equation

$$\frac{d \ln K}{d1/T} = -\frac{\Delta H^0}{R}. \qquad \text{[S8]}$$

CD and NMR spectroscopy. CD measurements were performed on an Aviv DS62 spectropolarimeter at 5.0 °C. Spectra were recorded with 50 μM HP35 in a 0.1 cm cuvette. Equilibrium unfolding transitions were measured at 222 nm with 5 μM HP35 in a 1 cm cuvette and evaluated according to Santoro and Bolen (6).

Proton NMR spectra were recorded on a Bruker Avance 600 MHz spectrometer at 25.0 °C and referenced to 2,2-dimethyl-2-silapentane-5-sulfonate at 0.0 ppm.

1. Fierz B, Reiner A, and Kiefhaber T (2009) Local conformational fluctuations in α-helices measured by fast triplet transfer. *Proc Natl Acad Sci USA* 106:1057–1062.
2. Hvidt A and Nielsen SO (1966) Hydrogen exchange in proteins. *Adv Prot Chem* 21:287–386.
3. Linderstrøm-Lang K (1955) Deuterium exchange between peptides and water. *Chem Soc Spec Publ* 2:1–20.
4. Graham R and Lewis JR (1978) Synthesis of 9-oxoxanthen-2-carboxylic acids. *J Chem Soc Perkin Trans 1* 876–881.
5. Pace CN (1986) Determination and analysis of urea and guanidine hydrochloride denaturation curves. *Method Enzymol* 131:266–280.
6. Santoro MM and Bolen DW (1988) Unfolding free energy changes determined by the linear extrapolation method. 1. Unfolding of phenylmethanesulfonyl alpha-chymotrypsin using different denaturants. *Biochemistry* 27:8063–8068.
7. McKnight CJ, Doering DS, Matsudaira PT, and Kim PS (1996) A thermostable 35-residue subdomain within villin headpiece *J Mol Biol* 260:126–134.
8. Gao J and Kelly JW (2008) Toward quantification of protein backbone hydrogen bonding energies: An energetic analysis of an amide-to-ester mutation in an α-helix within a protein. *Protein Sci* 17:1096-1101.

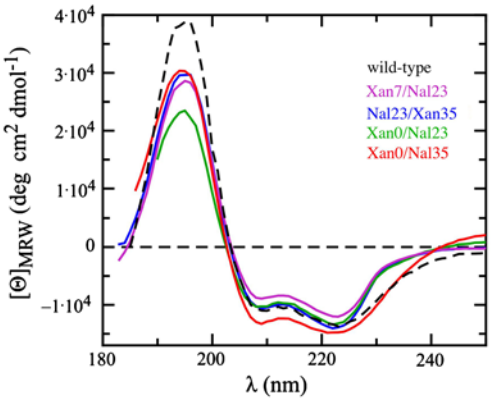

Fig. S1. Far-UV CD spectra of the different HP35 variants at 5.0 °C. The spectra are influenced by a positive CD band of naphthalene around 225 nm and by absorbance of Xan, which does not allow a quantitative comparison with the unlabeld wild-type protein. The spectrum of the Xan0/Nal35 variant is additionally influenced by the interaction between Xan and Nal (see Figs. 1 and 2). Measurements were performed in 10 mM potassium phosphate, pH 7.0. The spectrum of the wild-type protein was taken from ref. 7. In this case the solution additionally contained 150 mM NaCl and 500 μM EDTA.

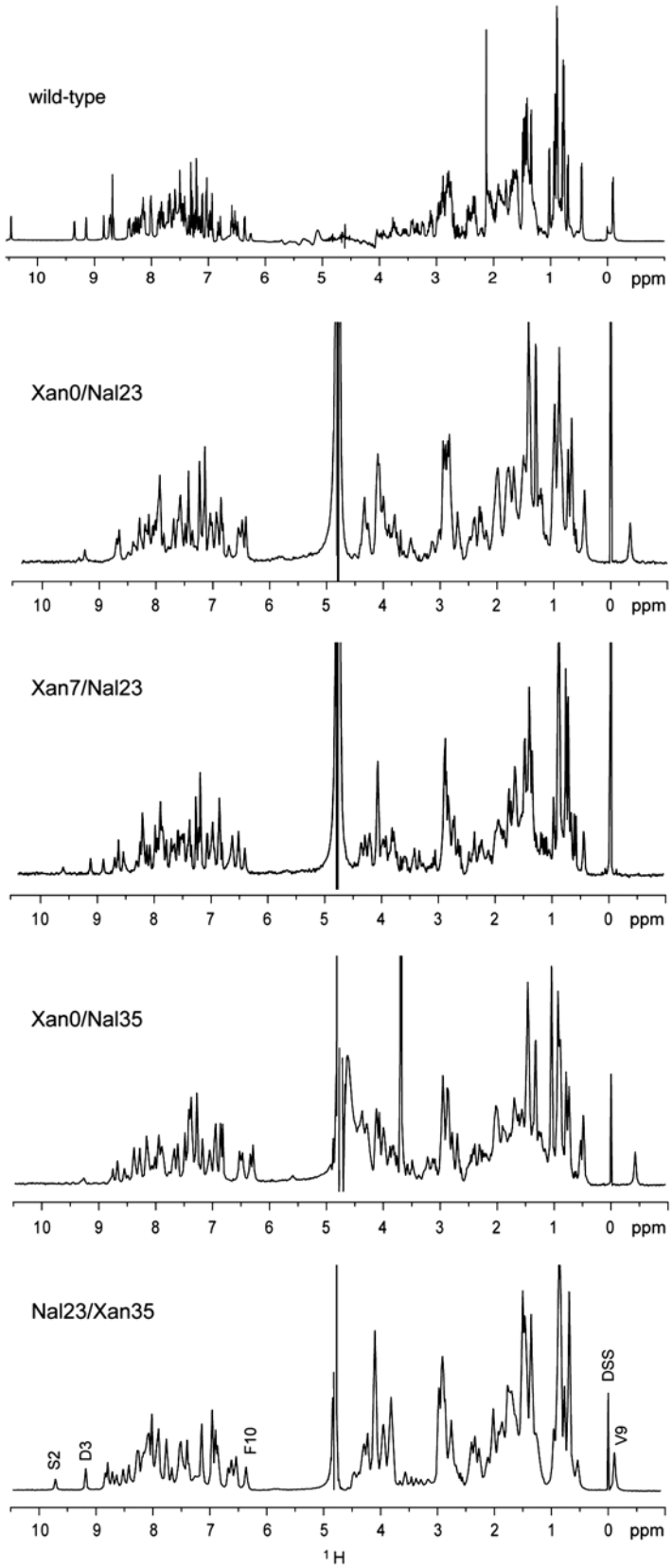

Fig. S2. One-dimensional ^{1}H NMR spectra of all HP35 variants in 5% (v/v) D_2O at 25 °C, pH 7.0. The assignment of the Ser2 and Asp3 amide protons, the aromatic side-chain proton of F10 and of the Val9 methyl group protons was confirmed by NOESY spectra (7). The spectra of the labeled variants contain additional contributions from Nal and Xan in the armomatic region and have the resonance of the Trp23 indole proton around 10.3 ppm missing, since Trp 23 was replaced by either Nal or Phe. The wild-type spectrum was taken from ref. 8.

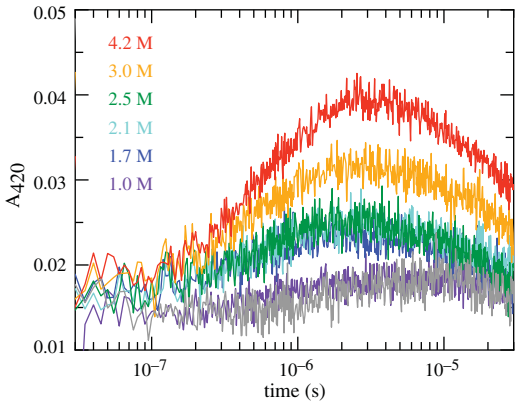

Fig. S3. TTET in the Xan0/Nal23 variant measured by the increase in the acceptor triplet absorbance at 420 nm at the indicated GdmCl concentrations at 5.0 °C. Data from the donor-only variant in 1.0 M GdmCl are shown in gray. The corresponding decays of the donor triplet absorption are shown in Fig. 2*A*. Measurements were performed in 10 mM potassium phosphate, pH 7.0.

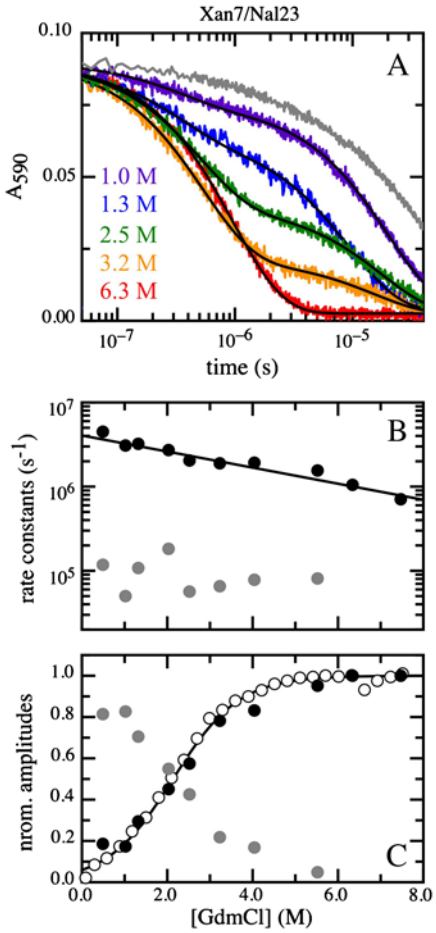

Fig. S4. TTET at different GdmCl concentrations in the HP35 Xan7/Nal23 variant at 5.0 °C. (*A*) Xan triplet decay curves measured by the absorbance change at 590 nm at the indicated GdmCl concentrations. For comparison, the intrinsic xanthone triplet lifetime in the native state measured in the Xan7 donor-only variant is shown in gray. The solid lines represent double exponential fits with rate constants shown in (*B*) and normalized amplitudes shown in (*C*) (see also Table S1). The fractions of unfolded molecules determined by CD-detected equilibrium unfolding transitions are additionally shown in (*C*) (open circles).

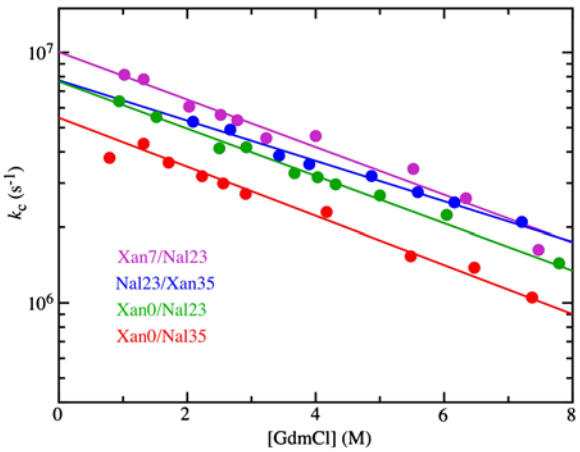

Fig. S5. Effect of GdmCl on the rate constant for loop formation (k_c) in the unfolded state of the different HP35 variants at 22.5 °C. Results of the linear fits are given in Table S1.

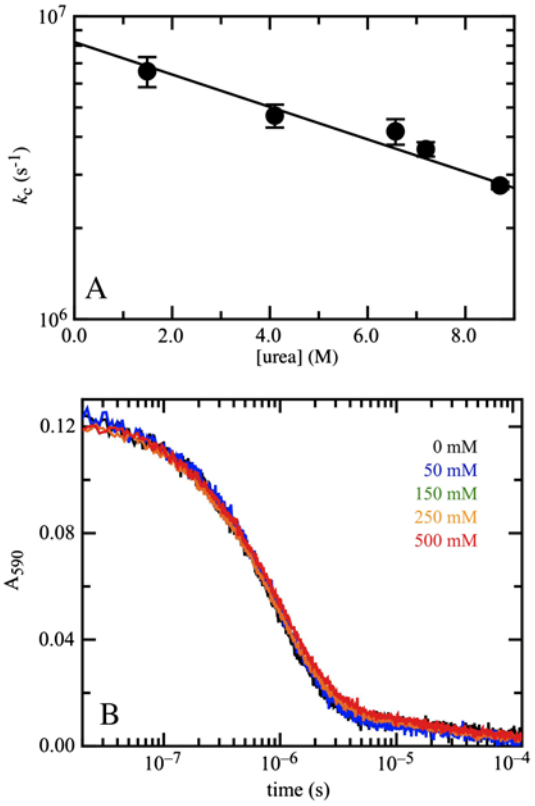

Fig. S6. (*A*) Effect of urea on the rate constants for loop formation in the unfolded state of the Xan0/Nal23 variant at 22.5 °C. The line represents a fit of the equation $\ln k_c = \ln k_c^0 + m_c[\text{GdmCl}]$ to the data with $k_c^0 = (8.2 \pm 0.8) \cdot 10^6$ s^{-1} and $m_c = 0.28 \pm 0.03$ (kJ/mol)/M. (*B*) X0/N23 contact formation in 8 M urea in the absence of salt (black line) and increasing concentrations of NaCl up to 500 mM (colored as indicated) at 5.0 °C.

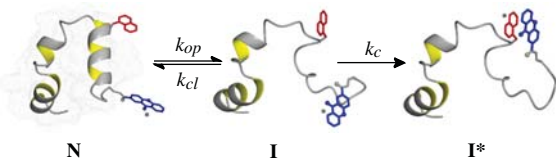

Scheme S1

Reiner et al. www.pnas.org/cgi/doi/10.1073/pnas.0910001107

Table S1. Stability and dynamics of TTET in the different HP35 variants

Variant	Stability* 5.0 °C		Loop formation in the unfolded state† 5.0 °C		22.5 °C		TTET in the native state‡ 5.0 °C		Activation parameters	
	ΔG_F^0 kJ/mol	m_{eq} (kJ/mol)/M	k_c^0 10^6 s^{-1}	m_c (kJ/mol)/M	k_c^0 10^6 s^{-1}	m_c (kJ/mol)/M	λ^0 10^6 s^{-1}	m (kJ/mol)/M	A 10^{10} s^{-1}	E_a kJ/mol
Xan0/Nal23	−6.4 ± 0.6	2.9 ± 0.3	2.7 ± 0.1	0.42 ± 0.03	7.7 ± 0.3	0.50 ± 0.02	<0.02	-	-	-
Xan7/Nal23	−6.4 ± 0.4	3.0 ± 0.2	4.0 ± 0.2	0.51 ± 0.02	10.0 ± 1.8	0.51 ± 0.03	<0.02	-	-	-
Xan0/Nal35	−8.3 ± 0.5	3.2 ± 0.2	2.9 ± 0.3	0.57 ± 0.08	5.5 ± 0.3	0.52 ± 0.03	>300	–	-	-
							23 ± 3	0.70 ± 0.1		
Nal23/Xan35	−7.0 ± 0.6	3.0 ± 0.2	3.2 ± 0.1	0.42 ± 0.01	7.7 ± 0.8	0.43 ± 0.02	5.9 ± 0.4	−1.8 ± 0.2	1.3 ± 0.6	17 ± 1
							1.1 ± 0.1	0.22 ± 0.13	75 ± 13	32 ± 1

*ΔG_F^0 and m_{eq}-values were determined in GdmCl-induced unfolding transitions at 5.0 °C (Fig. 2).

†Rate constants for loop formation in the unfolded state (k_c) were extrapolated to 0 M denaturant (k_c^0) (Fig. 2 and Figs. S4 and S5).

‡Apparent rate constants for native-state TTET were extrapolated to zero denaturant (λ^0); Arrhenius parameters were obtained from fitting the data shown in Fig. 3*A* to the equation $k = A \cdot \exp(-E_a/RT)$.